

Subsurface Topography and Geomagnetic Behavior: A New Perspective from Modelling Local Anomalies Mount Etna

Magnetic Terrain Effect and Paleomagnetism: New Evidence from Forward Modelling Mount Etna Unravels Large Local Magnetic Field Anomalies

Agnes E. Hendrickx, Cedric Thieulot, Lennart V. de Groot

Abstract

In the study of paleomagnetism the records of paleosecular variation (PSV) used are often obtained from volcanic lava flows. Obtaining reliable absolute paleomagnetic data from lava flows is therefore of eminent importance. However, this has over the years proven to be surprisingly difficult as samples from the same lava flow often show large within- and between-site dispersion, exceeding the admissible error from sampling and measuring. In this study, we will show that the Magnetic Terrain Effect(MTE) can account for a great deal of these anomalies. We conclude that in areas of highly magnetized rock, like lava flows, the topography of the underlying flow produces local magnetic anomalies in the magnetic field above the flow. Subsequently, these anomalies will be recorded in a lava flow deposited on top.

Here, we present a data-independent finite element model capable of simulating topographies and accurately predicting the magnetic field above highly magnetized rock. Using this forward model, code written in FORTRAN 90, we can adequately reproduce measurements taken at several sites on Mt. Etna (Italy) in 2018. High resolution Digital Elevation Models (DEMs) are used to obtain the local topographical data. The computed anomalies are strikingly similar to the measured results. The accuracy of the model relies mostly on how well the terrain, as measured in the field, is depicted by the DEM. The computed values of intensity deviations from the average are up to 8 μT (15%), inclination deviations up to 7° , and declination deviations up to 8° . These values compare very well to the measured intensity deviations from the average (IGRF) up to 7 μT , inclination deviations up to 8° , and declination deviations up to 20° on the Etna.

Since the underlying topography is often unknown, distinction between PSV or the MTE is near impossible. Our observations lead us to suggest that in rugged volcanic terrain an accurate paleomagnetic measurement of a lava flow can only be found by taking a sufficient amount of measurements of the same flow at different sites.

meer over model, topographien op meerdere manieren, case study Etna

1 Introduction

In the field of paleomagnetism, volcanic lava flows offer invaluable records of paleosecular variation (PSV) as they crystallize and 'freeze' a magnetic vector parallel to the geomagnetic field at the moment of their formation. The ability of volcanic rocks to acquire strong and stable thermoremanent magnetization (TRM) has lead to their recognition as a near-perfect recorder for the ancient magnetic field. Consequently, paleomagnetic data from lava flows have widespread scientific applications, including constraining the chronological framework for (archaeological) sites, tracking the evolution of the Earth's magnetic field, providing insight into tectonic evolution, and even informing volcanic hazard management strategies. Obtaining reliable absolute paleomagnetic data from lava flows is therefore of eminent importance.

However, the acquisition of reliable and accurate paleomagnetic data from lava flows has over the years proven to be surprisingly difficult. Samples from the same lava flow often show large within- and between-site dispersion, exceeding the admissible error from sampling and measuring (Castro & Brown, [1987]; Speranza et al., [2006]). Furthermore, magnetic vectors in freshly cooled volcanic rocks frequently deviate from expected or International Geomagnetic Reference Field (IGRF) values, with these discrepancies reported across various global locations, e.g. Italy, Hawaii, Japan, Mexico and the Canary Islands (Coe et al., [1978]; Herrero-Bervera & Valet, [2009]; Meyer & de Groot, [2023]; Mochizuki et al., [2004]; Speranza et al., [2006]; Urrutia-Fucugauchi et al., [2004]; Valet & Soler, [1999]).

These disparities have sparked decades-long debates questioning the overall reliability of paleomagnetism as a scientific method, requiring convoluted explanations to justify the recorded anomalies. Over the years, various hypotheses have been proposed to explain these discrepancies, including lock rotations (Nyblade et al., [1987]), local non-dipole geomagnetic fields (Coe et al., [1978]), large-scale crustal movements (Beck Jr, [1984]), differences in field and lab cooling rates (Biggin et al., [2007]; Hill & Shaw, [1999]), and intricate 'transdomain' processes (de Groot et al., [2013]). Nonetheless, most of these proposed explanations have either been discredited or have failed to fully account for the observed disparities (Baag et al., [1995]; de Groot et al., [2013]).

One proposition, the Magnetic Terrain Effect (MTE) hypothesis, suggest that irregular topography and high-intensity magnetization of the underlying rocks can locally deflect the ambient geomagnetic field, which in turn can be incorporated in a lava flow cooling above (Baag et al., [1995]; Meyer & de Groot, [2023]; Speranza et al., [2006]; Tanguy & Le Goff, [2004]; Valet & Soler, [1999]). This deflection arises from the reversed magnetic field generated by the magnetized terrain, a fact long recognized by those aware of compass distortions in volcanic areas. However, the MTE's significance in skewing paleomagnetic data has largely been overlooked or underestimated (Baag et al., [1995]; Meyer & de Groot, [2023]).

The potential influence of MTE on ambient magnetic fields was first put forward by Baag et al., [1995], demonstrating a link between topographic irregularities in Hawaii and deviations in magnetic field inclinations. However, these initial 2D models could not fully reconcile the magnitude of observed inclinations anomalies of up to 20° from IGRF. Despite this, they established a correlation between the terrain and magnetic anomalies, a finding that has since been supported by further research, both on the Canary Islands and on Mt. Etna (Meyer & de Groot, [2023]; Speranza et al., [2006]; Valet & Soler, [1999]). However, this research has remained largely theoretical. Previous research has eliminated the potential area-wide effect of the volcanic pile of Mt. Etna on the ambient magnetic field (Tanguy & Le Goff, [2004]), supporting the theory suggesting that significant local anomalies are likely caused by the flow just below of it (Baag et al., [1995]; Meyer & de Groot, [2023]; Speranza et al., [2006]; Tanguy & Le Goff, [2004]; Valet & Soler, [1999]).

Most recently, Meyer and de Groot, [2023] provided robust evidence for MTE, showing that magnetic field measurements above highly magnetized flows correlate with the underlying topography, with anomalies in inclination and intensity above ridges and gullies, deviating up to 8° in inclination and 15% in intensity from the IGRF. These findings underscore the need to consider MTE when interpreting paleomagnetic data. Part of the fieldwork conducted on Mount Etna in 2018 was specifically designed to measure the magnetic anomalies above volcanic terrain. Measurements were taken at six sites of different lava flows on various flanks of Mt. Etna (Figure 1) (Meyer & de Groot, [2023]). These

results reinforced the importance of considering MTE when interpreting paleomagnetic data from volcanic terrains.

MTE poses a threat to the reliability of a paleomagnetic record due to several reasons. First, since the ancient underlying terrain of a lava flow is unknown, distinction between dispersion due to PSV and MTE is often not possible (Baag et al., 1995). This issue is compounded by the fact that MTE-induced anomalies typically extend beyond 1 meter, rendering small-area sampling and strategies aimed at minimizing data scatter ineffective in mitigating their influence. . Furthermore, such strategies, when applied in complex volcanic terrains, may inadvertently introduce systematic biases into the PSV records—biases that are often subtle and difficult to uncover (Meyer & de Groot, 2023; Valet & Soler, 1999).

A systematic bias in both the inclination and intensity of paleomagnetic data were identified by Meyer and de Groot, 2023, who noted that, on average, measurements from young Etnean lava flows were approximately 2.8° in inclination and $6.9 \mu\text{T}$ in intensity lower than predicted by IGRF values. This underestimation was attributed to the MTE, particularly to the diminished magnetic fields within the depressions of the terrain, where new lava flows are likely to accumulate (Meyer & de Groot, 2023). Similarly, a consistent underestimation of inclination by about 3° has been documented in lava flows across the Northern Hemisphere over the last four centuries, suggesting a potential widespread influence of MTE (Pavón-Carrasco et al., 2016).

This evidence of systemic bias, possibly caused by MTE, highlights a pressing need for more sophisticated modeling techniques that can accurately predict the effects of MTE on the magnetization of volcanic rocks. In this research, we presents a three-dimensional, data-independent finite element model to simulate various topographies and calculate local magnetic anomalies above volcanic terrain. The model, validated against benchmarks and capable of representing a range of topographic features, from gullies on volcanic flanks to the integration of digital elevation models (DEMs). Finally, the MTE model was applied to reproduce the field sites of (Meyer & de Groot, 2023), allowing us to computed values to the measured anomalies in the field.

The MTE model can be used to explore the origins of these anomalies, identify terrain shapes most susceptible to them, and predict their impact on future paleomagnetic research conducted in similar areas. Furthermore, as these anomalies are embedded into any subsequent solidifying flow, they provide an opportunity to study the incorporation methods within any future layers atop the known topography of today. Hereby paving the way for even possible removal of the terrain effect from future paleomagnetic records. Additionally, it can be used to enhance the accuracy of global paleomagnetic models by estimating adequate scatter for research areas.

2 Methods

2.1 Governing equations

The governing equations of the MTE model focus on computing the magnetic field generated by magnetized matter, particularly volcanic rock, in the presence of the Earth's magnetic field. At any given point \mathbf{r} , the total magnetic field $\mathbf{B}_t(\mathbf{r})$ comprises the Earth's uniform magnetic field \mathbf{B}_0 and the anomalous field \mathbf{B}_a originating from the underlying magnetized matter.

The anomalous field is produced by the magnetized volcanic rock. As the rock cools, certain minerals become magnetic, aligning with the Earth's magnetic field, and upon further cooling, they retain this alignment as thermal remanence (TRM) (Tauxe, 2010). Considering these minerals as minuscule dipoles at a sufficient distance (i.e. outside of the source), the material's magnetization \mathbf{M} equates to its magnetic dipole moment \mathbf{m} per unit volume V (Reitz & Milford, 1960). This relationship allows for the magnetic field of a dipole ($\mathbf{B}_{dip}(\mathbf{r}) = \frac{\mu_0}{4\pi} \left[\frac{3\mathbf{r}(\mathbf{m}\cdot\mathbf{r})}{r^5} - \frac{\mathbf{m}}{r^3} \right]$) to be expressed as an integral over the volume of magnetization (Griffiths, 2013). Assuming a uniform magnetization across the volcanic flow simplifies calculations by discarding variations within the lava, thereby focusing on topographical influences. Additionally, it allows for the reduction of the volume integral to a surface integral (see appendix for

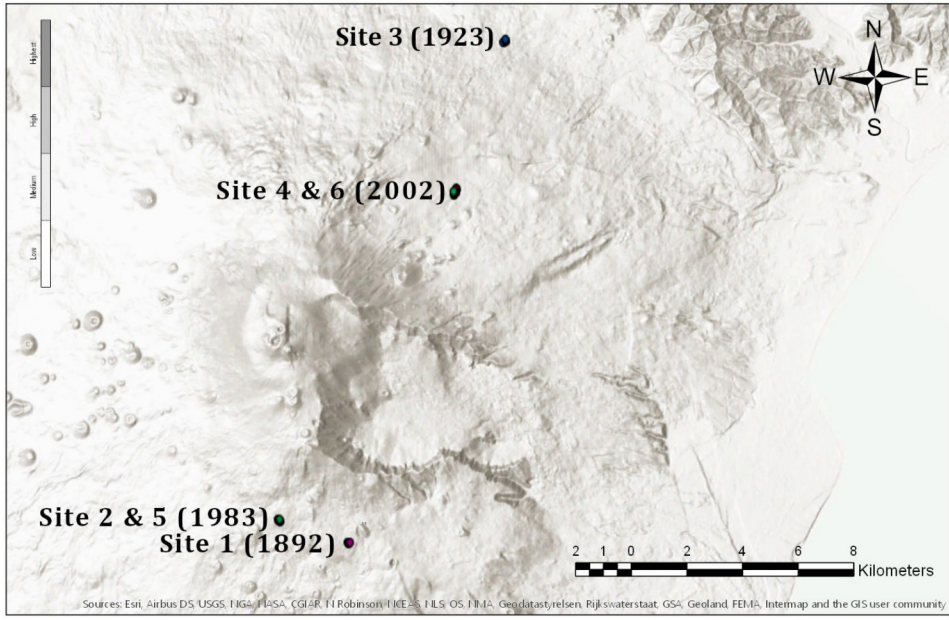


Figure 1: Location of the sites on different flows the various flanks of Mount Etna, site 2 & 5 and 4 & 6 are within close proximity. The age of the lava flow measured is displayed in brackets.

complete derivation), leading to the fundamental equation:

$$\mathbf{B}_t(\mathbf{r}) = \mathbf{B}_0 + \frac{\mu_0}{4\pi} \oint_S \frac{(\mathbf{M}(\mathbf{r}') \cdot \hat{\mathbf{n}})(\mathbf{r} - \mathbf{r}')}{|r - r'|^3} ds' \quad (1)$$

This equation reflects the magnetized body's surface contribution to the total field, where $\hat{\mathbf{n}}$ is the unit vector normal to the surface S and $\mathbf{r} - \mathbf{r}'$ represents the distance between the observation point and an element with surface ds' ??).

2.2 The computational approach

The computational approach of the MTE model utilizes Finite Element Modeling (FEM) to resolve the integral equations for the magnetic field. It involves creating a 3D domain tessellated into multiple elements, each representing a uniformly magnetized volume. The model explores the impact of the terrain's topography on the magnetic field through either an equation-based approximation or DEM-sourced elevation data.

The magnetic anomaly at an observation point \mathbf{P} is computed solving the surface integral, specified in the second part of the governing equation [1], for each domain element. The method, rooted in the works of Blakely, 1995; Bott, 1963 projects the magnetic effects of each element's face onto triangles and evaluates their influence based on proximity to \mathbf{P} . The cumulative magnetic effect of the domain is calculated, and then integrated with the Earth's reference field to determine the complete components of the magnetic field.

A key assumption is that the domain elements are sufficiently small, and their distance to \mathbf{P} is adequately large, especially for those elements nearest to the observation point. According to (Jackson, 1999), distance-related errors are trivial unless \mathbf{P} lies within a few molecular diameters of a uniformly magnetized element. This supposition is supported by empirical evidence from similar studies (Baag et al., 1995), affirming the model's validity for paleomagnetic applications.

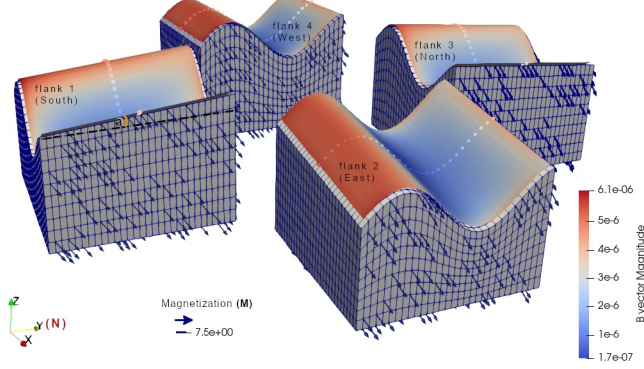


Figure 2: Flank simulation on the Etna. $(\mathbf{M}) = 7.5 \text{ A/m}$ (arrows). The slope (a in Figure, sf in code) is 0.15. The computations of the magnetic field (\mathbf{B}) above the flanks are done on a plane and path. The flanks are numbered as displayed. For visual display the size of the domain here is much smaller than in the test.

2.3 Model setup

2.3.1 Synthetic topography: Flank simulations

Given that the majority of lava flows are located on the flanks of volcanoes, simulating volcanic flanks is a relevant and intuitive starting point for our initial generic modeling setup. While the magnetization direction remains consistent, the dip direction of the surfaces on these flanks varies. To explore the impact of these variances, we established a model setup dedicated to flank simulations, as illustrated in Figure 2. In our approach, the flank topography is emulated using a sine approximation on a slope, with the sine function capturing the characteristic ridges and gullies of volcanic topography.

In these simulations, a wide range of parameters can be adjusted to investigate their influence on the magnetic field. These include the surface slope, the amplitude and wavelength of the sine function, and the angle between the sine wave's direction and either the x-axis or y-axis—depending on the flank, as depicted in Figure ??.

For alignment with our case study, parameter estimates aiming to replicate the ridges and gullies of Mount Etna were derived from aerial images and Digital Elevation Models (DEMs). The estimated amplitude, wavelength, and angle for the slope were 8m, 25m, and 6 °, respectively.

Flank simulations were done using a domain of 250x250x20m with 375x375x10 elements (per predetermined required parameters), with computation done a path of 47 points located one meter above the center of the domain. The sine wave was shifted to create the exact same topography underneath the path at the center of each flanks.

2.3.2 Mount Etna

To compare to the field measurements in this study, the uniform remnant magnetization intensity assigned to the matter was: 7.5 A/m. This value compares well with both the TRM found in samples taken from the lava flows in the field (Meyer & de Groot, 2023) and with previous paleomagnetic studies of Etnean lavas (Nicolosi et al., 2014); a bulk magnetization intensity of 8 A/m was measured, with values ranging between 5 and 13 A/m. However, both much lower and higher values have also been reported in other studies, 0.1-1 A/m and 20 A/m by (Speranza et al., 2006; Tanguy & Le Goff, 2004), respectively. Clearly displaying the large dispersion of the measurements or values of the magnetization in Etnean lavas. The inclination of the magnetization used in this study is 57°. This value was computed from Mount Etna's average latitude using the Geocentric Axial Dipole hypothesis, ($\tan I = 2 \tan(lat)$). The declination was assumed to be 0° (parallel to the present geomagnetic field) and from this the components of the magnetization were calculated. For alignment with our case study, parameter estimates aiming to replicate the ridges and gullies of Mount Etna were derived from aerial images and Digital Elevation Models (DEMs). The estimated amplitude, wavelength, and angle for the slope were 8m, 25m, and 6 °, respectively.

2.3.3 Topography from Digital Elevation Models at field paths

The 2x2m spatial resolution DEM ATA 2007-2008, [2010] is geo-referenced using the ROMA 40/EST - EPSG 3004 in Gauss–Boaga projection. We converted the 2m DEM to WGS84 UTM 33N in ArcGIS Pro using bilinear interpolation. This 2m DEM is publicly accessible through the web-sphere of SITR. While detailed information regarding data acquisition methods is absent, it is understood that the original data source was LiDAR. In contrast, the 5x5m spatial resolution DEM presented in Bisson et al., [2016] is geo-referenced using the WGS84 UTM 33N System, boasting a vertical accuracy with a root-mean-square-error of $\pm 0.24m$. This DEM is derived from data obtained using airborne LiDAR. Regarding the 5m DEM, it is stated that the DEM was obtained by resampling of an original 2m DEM using the nearest neighbors algorithm (Bisson et al., [2016]). Subsequently, they conclude that the vertical and horizontal accuracy of the original data is conserved. Both DEMs were cut to different sizes, ranging in spatial extent from 50x50 m to $\sim 2 \times 2\text{km}$ around the sites. While retaining the original 2m accuracy is commendable, working with a 5m DEM inherently restricts us to a 5m resolution, hence capping our potential accuracy. Despite multiple attempts, the original 2m DEM remained elusive, compelling this study to proceed with the 5m DEM.

To reproduce the field data, a path can be generated based on the GPS coordinates of field data by using the x & y coordinates from the field path, the height is computed at a constant value above the surface of the DEM. The GPS field data in this study was converted from decimal degrees to the WGS84 UTM 33N system to match the DEMs. The DEM cut's corner x- and y-coordinates were subtracted from the field coordinates, ensuring alignment. The height of the GPS placement on the measuring device, 2m above the surface (de Groot & de Groot, [2019]), was subtracted from the field data beforehand.

Two different reference fields were added to the computed values: The IGRF at the site or the average on the Etna at the moment of measuring (April 2018) and \mathbf{B}_{ref} . The latter is the computed mean of all field data from all paths at one site. Inputting the appropriate site (and path) details triggers an automatic retrieval of the relevant DEM, reference field, IGRF, magnetization, etc.

2.4 Visualisation

As our final objective is to compare the observed to the measured values, it is desirable to display the computed values in plots that include the field data points and the trajectory of the path. Therefore, the magnetic field above the flow and the height of the elevation will be plotted against the distance between the measurement points. Such plots are easily comparable on all slopes and at all sites. This does affect the reliability of the displayed topography in these plots; only if the path is perpendicular to the slope would this display the topography perfectly. Undoubtedly, this was not always possible or achieved in the field. However, as one of the selection criteria for the paths was for it to be perpendicular to the slope, we trust these plots to hold an accurate representation of the salient topographic features.

Discrepancies in height data between the DEM and field data are not uncommon. Multiple factors can contribute to such misfit, including inaccuracies in the field data or DEM, multiple coordinate conversions, potential discrepancies between coordinate systems, and more. To quantify this disparity, we computed the height difference across all field path points for both DEMs, averaged them, and then adjusted the field measurement paths accordingly (refer to the code for exact values). Ideally, one constant offset would be applicable across all sites, but this wasn't the reality. Nonetheless, our primary concern is aligning heights for accurate comparison. We aren't particularly invested in identifying the genuine offset or its root cause. Hence, applied offsets might vary by site and were deducted from all field measurement points prior to plotting. Any height offset between values of the 2 and 5m DEM were also compensated in similar fashion.

Additionally, in some instances, a clear spatial misalignment was evident, with the field topography and DEM aligning better after a minor adjustment. Any adjustments made for visualization clarity were applied manually, grounded in enhancing the congruence of topographic features. Whenever modifications were made, the figures are labeled as "shifted", and the original unaltered plots can be found in the appended section.